

An Electrically Tunable Focusing Pico-Projector Adopting a Liquid Crystal Lens

This content has been downloaded from IOPscience. Please scroll down to see the full text.

2010 Jpn. J. Appl. Phys. 49 102502

(<http://iopscience.iop.org/1347-4065/49/10R/102502>)

View [the table of contents for this issue](#), or go to the [journal homepage](#) for more

Download details:

IP Address: 140.113.38.11

This content was downloaded on 25/04/2014 at 06:19

Please note that [terms and conditions apply](#).

An Electrically Tunable Focusing Pico-Projector Adopting a Liquid Crystal Lens

Hung-Chun Lin and Yi-Hsin Lin*

Department of Photonics, National Chiao Tung University, Hsinchu, Taiwan 30010, R.O.C.

Received March 23, 2010; accepted July 10, 2010; published online October 20, 2010

An electrically tunable pico-projector adopting a liquid crystal (LC) lens as an active optical element is demonstrated. The focal length of this pico-projector is electrically tunable from 350 to 14 cm and the tunable range is even wider than that of a manually focused pico-projector. The response times of turn-on and turn-off are approximately 313 and 880 ms, respectively. In addition, the location of the projection lens can affect the electrically tunable range of the system. A small shift of the projection lens results in the large tunable focusing range of the pico-projector and a tunable focusing range is determined by the LC lens. The optical analysis is also discussed. This concept can even be applied to design other electrically auto focusing pico-projectors based on other optical elements such as liquid lenses and spatial light modulators.

© 2010 The Japan Society of Applied Physics

DOI: 10.1143/JJAP.49.102502

1. Introduction

Pico-projectors can generate a portable instant screen for pocket devices and are important in many applications such as cell phones, digital cameras, and tablet personal computers (PCs).¹⁻³⁾ There are three kinds of pico-projectors in general: liquid-crystal-on-silicon (LCOS)-based pico-projectors, digital light processing (DLP)-based pico-projectors, and laser-scanning pico-projectors.¹⁻³⁾ Unlike laser-scanning pico-projectors, LCOS-based systems and DLP-based systems require focusing elements or projection lenses for focusing the projected image on the screen for observation. By changing the position of the projection lens, the focal length in the LCOS- or DLP-based pico-projectors is manually switchable. Generally, manually focused pico-projectors are bulky because of the packaging of the set of projection lenses and the manual switching device. Therefore, in order to obtain a pico-projector with reduced weight and electrically tunable focusing properties, we can replace the manually switchable projection lenses with electrically tunable lenses. To achieve the electrically tunable focusing of pico-projectors, electrically tunable focusing lenses can be adopted such as liquid lenses and liquid crystal (LC) lenses.⁴⁻²⁷⁾ In this study, to demonstrate this concept, we keep the projection lens in the pico-projector and use a LC lens as an active optical element. We then demonstrate an electrically tunable focusing LCOS-based pico-projector by using a LC lens as an active optical element. Without attaching a polarizer on the LC lens, the optical efficiency is not decreased by the polarizer. The electrically tunable range of the image distance of the proposed pico-projector is approximately 350 to 14 cm and the response time is approximately 1.2 s. The tunable range of the focal length of the pico-projector also depends on the position of the projection lens. The image performance of the electrically tunable focusing pico-projector is demonstrated.

2. Structure and Operating Principles

Figure 1(a) illustrates the structure of the electrically tunable pico-projector using a LC lens as an active optical element. In Fig. 1(a), the white light from a light-emitting diode (LED; XRE-Q5 CREE) passes through a relay lens to obtain a beam with uniform irradiance. A pre-polarizer and a polarizing beam splitter (PBS) are used for obtaining the

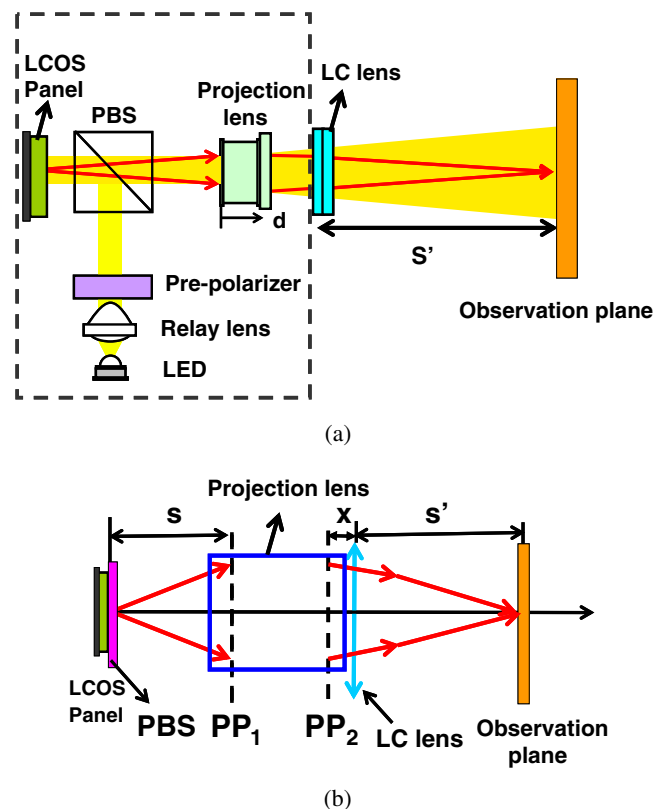


Fig. 1. (Color online) Structure of the projection system of an electrically tunable focusing pico-projector. (b) Schematic of the effective optical system of (a). PP_1 and PP_2 are the two principal planes of the projection lens.

crossed polarization of light with a high extinction ratio when the light is incident to and then reflected by a reflective LCOS panel. We use a projection lens to project the image from the LCOS panel. By controlling the focal length of the LC lens at different voltages, the location of the focused and projected image or the image distance (s') can be electrically adjusted. The projected image is then observed on the observation plane. Conventional LC lenses require polarizers owing to the polarization-dependent lens properties. Since the light passing through the projection lens is linearly polarized in LCOS-based pico-projectors, we do not attach any extra polarizer on the LC lens. At $V = 0$, the focal length of the LC lens is infinity. The image distance of the whole projection system is determined by the projection lens

*E-mail address: yilin@mail.nctu.edu.tw

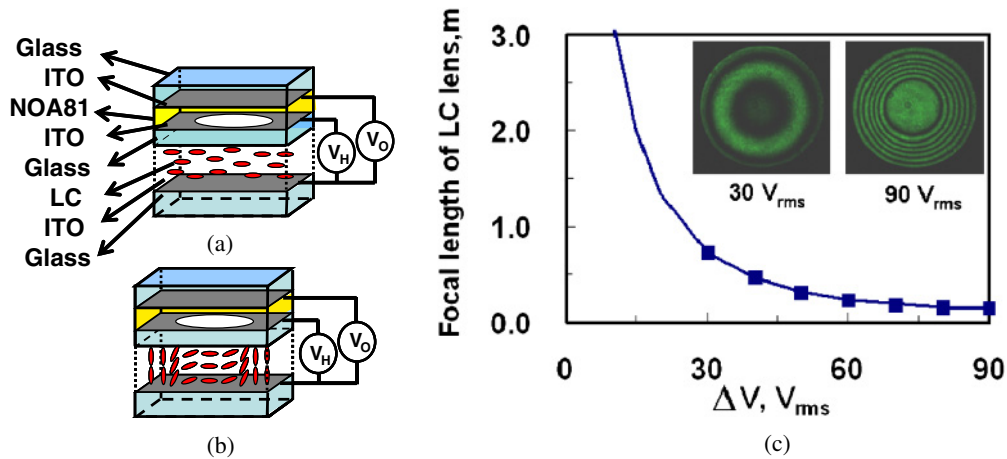


Fig. 2. (Color online) Structure and operating principles of the LC lens in the (a) voltage-off state and (b) voltage-on state. (c) Measured voltage-dependent focal length of LC lens. The insets are images of the LC lens under crossed polarizers at 30 and 90 V_{rms} . The rubbing direction was 45° with respect to one polarizer. $V_H = 90 V_{rms}$. $\lambda = 532$ nm.

only. Typical pico-projectors do not have a LC lens, and the image plane is manually adjusted by varying the distance (d) of the projection lens. The effective optical system of Fig. 1(a) is depicted in Fig. 1(b). The objective image is generated by the LCOS panel and then is imaged on the observation plane by both the projection lens and the LC lens. PP_1 and PP_2 are the two principal planes of the projection lens. When the position of the projection lens changes by a distance of d , the objective distance between the LCOS panel and principal plane PP_1 of the projection lens is $(s + d)$, and the distance between the LC lens and principal plane PP_2 of the projection lens is $(x - d)$. The focal lengths of the projection lens and LC lens are denoted as f_{pj} and f_{LC} , respectively. After the first image is formed by the projection lens, we can assume that the distance between the LC lens and the first image is p . According to the image equation, first image formed by the projection lens and second image formed by the LC lens can be expressed as²⁸⁾

$$\frac{1}{f_{pj}} = \frac{1}{s + d} + \frac{1}{x - d + p} \quad (1)$$

$$\frac{1}{f_{LC}} = -\frac{1}{p} + \frac{1}{s'}. \quad (2)$$

We can combine eqs. (1) and (2) by eliminating p to obtain eq. (3):

$$s'(f_{LC}(V), d) = \frac{f_{LC}(V) \cdot \left[\frac{f_{pj} \cdot (s + d)}{(s + d) - f_{pj}} - (x - d) \right]}{f_{LC}(V) + \frac{f_{pj} \cdot (s + d)}{(s + d) - f_{pj}} - (x - d)}, \quad (3)$$

where $f_{LC}(V)$ is the voltage-dependent focal length of the LC lens. In eq. (3), s' depends on the focal length of the LC lens at a fixed d . Therefore, the imaging plane of the pico-projection system is electrically tunable.

3. Experiment and Results

To demonstrate the concept of the proposed pico-projector, a commercial LCOS-based pico-projector (Himax HX7027-3W50-May), which is manually focused, was adopted. A LC lens was attached on a projection lens whose aperture size

was 11.28 mm. The structure of the LC lens was based on two-voltage structure as shown in Figs. 2(a) and 2(b).^{25,26)} The structure of the LC lens consists of three indium tin oxide (ITO) glass substrates of thickness 0.7 mm, a polymeric layer of NOA81 (Norland Optical Adhesive) with a thickness of 35 μm , and a LC layer with a thickness of 25 μm . The ITO layer of the middle ITO glass substrate was etched with a hole pattern within a diameter of 2 mm in order to provide an inhomogeneous electric field to the LC directors, and the opposite side of this ITO glass substrate was coated with a mechanically buffed poly(vinyl alcohol) (PVA) layer to align the LC directors. The bottom ITO glass substrate was also coated with an alignment layer with mechanically buffed polyimide layer. The rubbing directions of the two alignment layers are anti-parallel. The MLC-2070 nematic LC mixture (Merck, $\Delta n = 0.26$ for $\lambda = 589.3$ nm at 20°C) was used. The voltage applied between the hole-patterned ITO layer and the bottom ITO layer was fixed and was defined as the holding voltage (V_H). The other applied voltage was controllable and was defined as the operating voltage (V_O). The main purpose of the holding voltage is to first generate a phase profile of a positive lens, and then the phase profile is adjusted by varying the operating voltage. In this way, the focal length of the LC lens is positive and electrically tunable with good imaging properties. We define the difference between V_H and V_O as $\Delta V (= V_H - V_O)$. Figure 2(c) is the measured voltage-dependent focal length of the LC lens with a fixed $V_H = 90 V_{rms}$. In the experiments, a laser diode with a wavelength (λ) of 532 nm was used as a light source. The measured focal length of the LC lens can be switched from infinity to 14.46 cm. The insets of Fig. 2(c) are images of the LC lens at $\Delta V = 30$ and 90 V_{rms} under the crossed polarizers when the rubbing direction of the LC lens was 45° with respect to one of the polarizers. From the insets, the phase profiles of the LC lens, consisting of concentric circles, are symmetric and uniform, which indicates high image quality. In addition, more rings in the insets indicate a smaller focal length of the LC lens. The long focal length ($V < 30 V_{rms}$) of the LC lens cannot easily be determined by the number of concentric circular rings. However, a typical technique based on laser beam profiles,

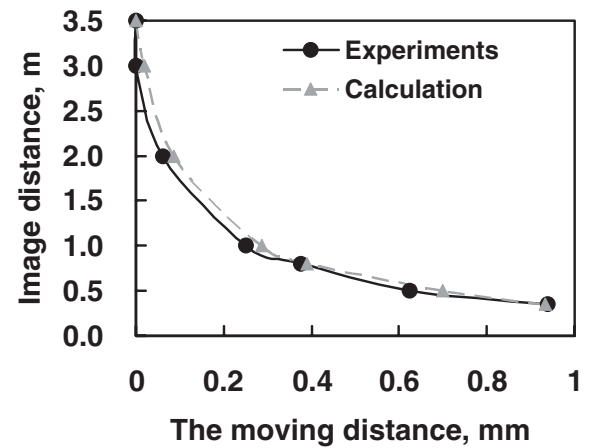
such as the knife-edge technique, can enable us to measure the waist of the beam and thus to determine the focal length of the LC lens. The measured response time was 880 ms when the operating voltage was switched from 90 to 0 V_{rms} , and was 313 ms when the operating voltage was switched from 0 to 90 V_{rms} .

We first measured the manual focusing properties of the pico-projector. We measured the image distance [i.e., s' in Figs. 1(a) and 1(b)] of a focusing image as a function of the moving distance of the projection lens [the moving direction is depicted in Fig. 1(a)] while no voltage was applied to the LC lens. In the experiments, we input an image of a resolution chart with a spatial frequency of 0.25 line pairs per millimeter (lp/mm) to the LCOS panel. The projected image was observed and we recorded the image distance [i.e., s' in Figs. 1(a) and 1(b)] when the contrast ratio of the projected image of the resolution chart was maximal. The measured results are shown in Fig. 3(a). The pico-projector was manually focused from an image distance of 350 to 35 cm when we moved the projection lens from 0 to 0.94 mm. The image distance decreases when we increase the moving distance of the projection lens. Using eq. (3), we can calculate the image distance of a manually focusing pico-projector. In eq. (3), $f_{\text{LC}}(V)$ is infinity and the moving distance of the projection lens is less than 1 mm (i.e., $d \ll x$ and $d \ll s$). Equation (3) can be rewritten as

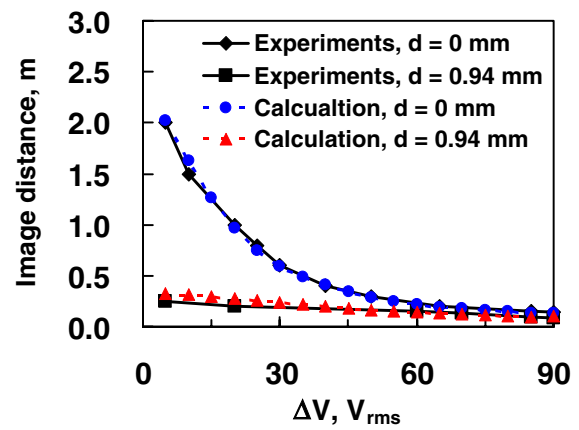
$$s'_m(d) = \frac{f_{\text{pj}} \cdot (s + d)}{(s + d) - f_{\text{pj}}} - (x - d). \quad (4)$$

The calculated results (triangles) are also plotted in Fig. 3(a), which were obtained by substituting the experimental parameters $s = 20$ mm, $x = 11$ mm, and $f_{\text{pj}} = 19.95$ mm into eq. (3). The calculated results agree with the experimental results.

To realize the electrically tunable focusing pico-projector, we measured the image distance (s') of a focusing image as a function of the applied voltage ΔV of the LC lens ($V_H = 90 V_{\text{rms}}$) while the location of the projection lens was fixed at $d = 0$ and 0.94 mm. The measured results are shown in Fig. 3(b). In Fig. 3(b), the image distance decreases with increasing ΔV . The image distance was tunable from 350 to 14 cm at $d = 0$ and from 35 to 9 cm at $d = 0.94$ mm when ΔV was increased from 0 to 90 V_{rms} . Therefore, using an electrically tunable focusing LC lens as an active imaging element, the manually operated pico-projector becomes an electrically focused pico-projector at a fixed d . The minimal focused image distance of the electrically tunable focusing pico-projector can even be made shorter than that of the manually operated pico-projector. This is because the wave after passing through the projection lens is nearly a plane wave at a small d , and then the LC lens is an effective phase modulator of the curvature of such a plane wave. As a result, the change of the image distance is large and limited by the LC lens power when a voltage is applied to the LC lens. Comparing Fig. 3(a) with Fig. 3(b), the position of the projection lens can determine the initial location of the image plane at $\Delta V = 0$, and the image plane can be adjusted by the LC lens when we apply voltage to the LC lens. The longer the image distance set by the projection lens, the larger the electrically tunable range that can be obtained by using the LC lens.



(a)



(b)

Fig. 3. (Color online) (a) Image distance as a function of the moving distance of the projection lens when no voltage is applied to the LC lens. (b) Image distance as a function of ΔV . $V_H = 90 V_{\text{rms}}$.

4. Discussion

In order to further investigate the tunable focusing range of the electrically tunable pico-projector, the results calculated using eq. (3) at $d = 0$ and 0.94 mm are plotted in Fig. 3(b). The calculated results agree with the experimental results. To discuss the results in Fig. 3(b), we replace eq. (3) with eq. (4), and then eq. (3) can be expressed as

$$s'(f_{\text{LC}}(V), d) = \frac{f_{\text{LC}}(V) \cdot s'_m(d)}{f_{\text{LC}}(V) + s'_m(d)}. \quad (5)$$

We further rearrange eq. (5) to give

$$s'(f_{\text{LC}}(V), d) = s'_m(d) \cdot \left[\frac{1 + s'_m(d)}{f_{\text{LC}}(V)} \right]^{-1}. \quad (6)$$

When $s'_m(d) \gg f_{\text{LC}}(V)$, $s'(f_{\text{LC}}(V), d)$ approximately equals $f_{\text{LC}}(V)$. This means that the image distance is electrically tunable and is equal to the focal length of the LC lens, as shown by the results for $d = 0$ in Fig. 3(b). This is because the wavefront of the incident light to the LC lens is almost planar after passing through the projection lens when $s'_m(d) \gg f_{\text{LC}}(V)$. Thus, the focal length is determined by the focal length of the LC lens. When $s'_m(d) \ll f_{\text{LC}}(V)$, $s'(f_{\text{LC}}(V), d)$ approximately equals $s'_m(d)$. This indicates that



Fig. 4. (Color online) (a) Image obtained from the manually focusing pico-projector without the LC lens. $d = 0.625$ mm and $s' = 50$ cm. (b) Images obtained from electrically tunable focusing pico-projector at (b) $V_o = V_H = 0$ and (c) $V_o = 43$ V_{rms} and $V_H = 90$ V_{rms}. $d = 0$ and $s' = 50$ cm.

the image distance is mainly determined by the projection lens and that we can only adjust the focal length slightly using the LC lens, as shown by the results for $d = 0.94$ mm in Fig. 3(b).

Figures 4(a)–4(c) show the image quality of the manually focusing pico-projector and the electrically tunable focusing pico-projector when we input a portrait to the LCOS panel. In order to keep the same aperture of the system, the case shown in Fig. 4(a), we removed the LC lens but we placed an aperture stop of 2 mm diameter to replace the LC lens with an aperture of 2 mm. We then adjusted the location of the projection lens until the image was clear when the image distance was 50 cm. For Figs. 4(b) and 4(c), we removed the aperture stop and the LC lens was reattached on the pico-projector. The images were observed without and with an applied voltage at an image distance of 50 cm at $d = 0$. In Fig. 4(c), the pico-projector with the LC lens indeed shows a good electrically tunable performance. In Figs. 4(a) and 4(c), the brightness of the focused image did not change significantly when the LC lens was used as an active optical element. This is because we did not attach an extra polarizer to the LC lens since the polarization of the projected light from the LCOS-based projection system was linearly polarized. However, the brightness still decreases by approximately 17% because of the multiple reflections in the multilayer structure, and the absorption resulting from the alignment layer and the ITO layers. The anti-reflection coating can improve the brightness of the projected image. In addition, the aperture mismatch between the projection lens (~ 11.28 mm) and the LC lens (~ 2 mm) can also degrade the brightness of the image and also cause vignetting. We can reduce this by enlarging the aperture of the LC lens.

The wavelength is also an important factor when using the LC lens owing to the wavelength-dependent birefringence and dispersion of LCs. In the measurement, the focal length of the LC lens changes from 14.5 cm for a wavelength of 650 nm to 11.6 cm for a wavelength of 450 nm. We also measured the on-axis optical performance of the LC lens at different wavelengths using equipment to measure the modulation transfer function (MTF; Trioptics ImageMaster HR). The MTF of the target is defined as the ratio of the difference between the maximal and minimal luminances to the sum of the maximal and the minimal luminances at different spatial frequencies.²⁸⁾ In order to compare the imaging results, we first measured the MTF of a commercial

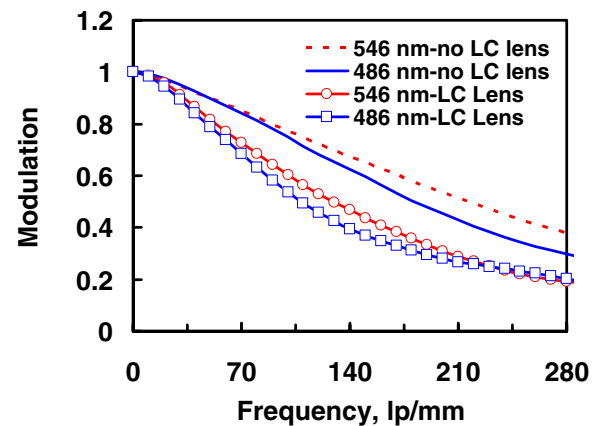


Fig. 5. (Color online) Modulation transfer function of the LC lens (open red circles and open blue squares) and lens module (red dotted line and blue solid line) at wavelengths of 546 and 486 nm. The voltage of the LC lens (ΔV) was 77 V_{rms}. The unit lp/mm stands for line pairs per millimeter.

lens module (Largan Precision; effective focal length = 4.73 mm) for an image sensor of 5 megapixels and then we measured the MTF of the lens module with the LC lens. The MTF or the modulation as a function of spatial frequency at different wavelengths is shown in Fig. 5. In Fig. 5, the MTFs of the lens module at different wavelengths are slightly different owing to the dispersion properties. After attaching the LC lens on the lens module, the MTFs of the system are smaller than those of the lens module. That means that the image quality degrades slightly from the average modulation of ~ 0.65 to that of ~ 0.44 at 140 lp/mm owing to the LC lens. In Fig. 5, the dispersion properties of the system consisting of the LC lens and the lens module are similar to those of the lens module. The modulation of the LC lens attached on the lens module is ~ 0.47 at 546 nm and ~ 0.40 at 486 nm. The dispersion of the LC lens does not affect the image quality markedly as we can see in Fig. 4. The high image quality of the LC lens is because of the paraboloid-like phase profile of the LC lens.

5. Conclusions

We have demonstrated an electrically tunable pico-projector by adopting a LC lens as an active optical element. The brightness of the projected image does not decrease markedly compared with what because no extra polarizer is used. The focal length of the system can be electrically

tunable from 350 to 14 cm and the tunable range is even wider than that of a manually focused pico-projector. The response time is approximately 1.2 s. However, the location of the projection lens can affect the electrically tunable range of the system. A small shift of the projection lens results in a large tunable focusing range of the pico-projector, and the tunable focusing range is determined by the LC lens. A large shift of the projection lens results in a small tunable focal length. The concept we proposed in this paper can also be applied to other electrically tunable focusing optical devices as active optical elements in pico-projectors, such LC lens with different structures, liquid lenses, and spatial light modulators.⁴⁻¹⁰ We believe that the achievements of this study open a new window for electrically tunable focusing pico-projectors.

Acknowledgements

The pico-projectors were sponsored by Himax Display Inc. The authors are indebted to Dr. Kuan-Hsu Fan-Chiang (Himax Display Inc.), Dr. Jinn-Chou Yoo (Shinyoptics Corp.), and Dr. David Chao (Young Optics Inc.), Dr. Yung-Hsun Wu (Chimei-Innolux Corp.), and Mr. Chuan-Chung Chang (ITRI) for technical support and discussions. This research was supported by the National Science Council (NSC) in Taiwan under contract No. 98-2112-M-009-017-MY3.

- 1) D. Armitage, I. Underwood, and S. T. Wu: *Introduction to Microdisplays* (Wiley, Chichester, U.K., 2006) p. 307.
- 2) E. H. Stupp and M. S. Brennessoltz: *Projection Displays* (Wiley, Chichester, U.K., 1999).

- 3) J. W. Pan, S. H. Tu, C. M. Wang, and J. Y. Chang: *Appl. Opt.* **47** (2008) 3406.
- 4) B. Berge and J. Peseux: *Eur. Phys. J. E* **3** (2000) 159.
- 5) S. Kuiper and H. W. Hendriks: *Appl. Phys. Lett.* **85** (2004) 1128.
- 6) B. H. W. Hendriks, S. Kuiper, M. A. J. van As, C. A. Renders, and T. W. Tukker: *Opt. Rev.* **12** (2005) 255.
- 7) Y. H. Lin, H. Ren, Y. H. Wu, S. T. Wu, Y. Zhao, J. Fang, and H. C. Lin: *Opt. Express* **16** (2008) 17591.
- 8) H. Ren and S. T. Wu: *Opt. Express* **15** (2007) 5931.
- 9) S. Sato: *Jpn. J. Appl. Phys.* **18** (1979) 1679.
- 10) T. Nose and S. Sato: *Liq. Cryst.* **5** (1989) 1425.
- 11) N. A. Riza and M. C. Dejule: *Opt. Lett.* **19** (1994) 1013.
- 12) W. W. Chan and S. T. Kowel: *Appl. Opt.* **36** (1997) 8958.
- 13) V. V. Presnyakov, K. E. Asatryan, T. V. Galstian, and A. Tork: *Opt. Express* **10** (2002) 865.
- 14) H. S. Ji, J. H. Kim, and S. Kumar: *Opt. Lett.* **28** (2003) 1147.
- 15) Y. H. Fan, H. Ren, X. Liang, H. Wang, and S. T. Wu: *J. Disp. Technol.* **1** (2005) 151.
- 16) H. Ren, Y. H. Lin, and S. T. Wu: *Opt. Commun.* **261** (2006) 296.
- 17) G. Li, P. Valley, P. Ayras, D. L. Mathine, S. Honkanen, and N. Peyghambarian: *Appl. Phys. Lett.* **90** (2007) 111105.
- 18) B. Wang, M. Ye, M. Honma, T. Nose, and S. Sato: *Jpn. J. Appl. Phys.* **41** (2002) L1232.
- 19) M. Ye and S. Sato: *Jpn. J. Appl. Phys.* **41** (2002) L571.
- 20) Y. H. Lin, H. W. Ren, K. H. Fan-Chiang, W. K. Choi, S. Gauza, X. Y. Zhu, and S. T. Wu: *Jpn. J. Appl. Phys.* **44** (2005) 243.
- 21) H. Ren and S. T. Wu: *Appl. Phys. Lett.* **82** (2003) 22.
- 22) H. Ren, Y. H. Fan, S. Gauza, and S. T. Wu: *Appl. Phys. Lett.* **84** (2004) 4789.
- 23) B. Wang, M. Ye, and S. Sato: *Opt. Commun.* **250** (2005) 266.
- 24) H. Ren, D. W. Fox, B. Wu, and S.-T. Wu: *Opt. Express* **15** (2007) 11328.
- 25) M. Ye, B. Wang, and S. Sato: *Appl. Opt.* **43** (2004) 6407.
- 26) B. Wang, M. Ye, and S. Sato: *IEEE Photonics Technol. Lett.* **18** (2006) 79.
- 27) M. Ye, B. Wang, M. Kawamura, and S. Sato: *Jpn. J. Appl. Phys.* **46** (2007) 6776.
- 28) W. J. Smith: *Modern Optical Engineering* (McGraw-Hill, New York, 2008) 4th ed., p. 35.